

CURVATURE EFFECT IN STRUCTURED GRB JETS

J. DYKS^{1,2}, BING ZHANG¹, AND Y. Z. FAN^{1,3,4}¹ Physics Department, University of Nevada Las Vegas, NV, USA² Centrum Astronomiczne im. M. Kopernika PAN, Toruń, Poland³ Purple Mountain Observatory, Chinese Academy of Sciences, Nanjing 210008, China⁴ National Astronomical Observatories, Chinese Academy of Sciences, Beijing, 100012, China

Draft version February 5, 2008

ABSTRACT

We study the influence of jet structure on the curvature effect in a GRB-lightcurve. Using a simple model of jet emissivity, we numerically calculate lightcurves for a short flash from a relativistic outflow having various profiles of the Lorentz factor and outflowing energy density (gaussian, core+power-law). We find that for “on-beam” viewing geometry, with the line of sight passing through the bright core of the outflow, the shape of the lightcurve practically does not depend on the jet structure, initially following the temporal slope $2 + \delta$, where δ is the spectral index. When the viewing angle is larger than the core, the light curve decaying slope is shallower. We discuss the implications of our results for the *Swift* data.

Subject headings: gamma rays: bursts — gamma rays: theory

1. INTRODUCTION

Recent *Swift* observations of gamma-ray burst afterglows (Tagliaferri et al. 2005; Chincarini et al. 2005; Nousek et al. 2005; O’Brien et al. 2005) revealed very fast drops of X-ray flux a few hundred seconds after the trigger time. The rapid decay is usually also followed with the X-ray flares (Burrows et al. 2005; O’Brien et al. 2005). A possible mechanism of this phenomenon is a sudden decrease of jet’s emissivity (see Zhang et al. 2005 for more comprehensive discussion of possible scenarios). For a curved front surface of a jet the turn-off is perceived by an observer as a fast, yet not abrupt, decrease of flux, because the simultaneous drop of emissivity at different angles θ from the line of sight is perceived at different moments. For uniform properties of the jet, and in the absence of further complicating factors, the temporal slope α of a lightcurve resulting from such a “curvature effect” is equal to $2 + \delta$, where δ is the spectral index and the conventions $F_\nu \propto t^{-\alpha}$ and $F_\nu \propto \nu^{-\delta}$ are assumed (Kumar & Panaitescu 2000; Fan & Wei 2005; Zhang et al. 2005; Panaitescu et al. 2005).

In addition to the spectral properties of emitted radiation, the structure of the jet, i.e. the variation of jet properties as a function of the angle θ from the jet axis, may influence the observed lightcurve – an issue addressed in many recent investigations (e.g. Zhang & Mészáros 2002; Rossi et al. 2002; Wei & Jin 2003; Kumar & Granot 2003; Granot & Kumar 2003; Salmonson 2003; Zhang et al. 2004; Yamazaki et al. 2005). During the curvature effect, an observer receives radiation emitted from different regions of the outflow (different θ). Therefore, an interesting question is whether the curvature effect depends on the unknown jet structure. The main purpose of this Letter is to address this question.

2. CALCULATION METHOD

To calculate the lightcurves we use a three dimensional code which rigorously takes into account all kinematic effects that affect the observed flux (eg. Doppler

boost, propagation time delays) in the way described by Salmonson (2003). To minimize the number of parameters involved, the curvature effect is studied for a short flash, with emission lasting between \tilde{t}_{init} and $\tilde{t}_{\text{off}} = 1.05\tilde{t}_{\text{init}}$ in the frame of the central source (we take $\tilde{t}_{\text{init}} = 10^{14}$ cm/c, where c is the speed of light). This is the typical internal shock radius (Rees & Mészáros 1994), at which the dynamics of the outflow evolves negligibly. At the time \tilde{t}_{init} the outflow is located at the radial distance $r_{\text{init}} = \beta(\theta)\tilde{t}_{\text{init}}$, where $\vec{\beta} = \vec{v}/c$ is the velocity of the outflow at the angle θ from the jet axis, and $\beta = |\vec{\beta}|$. This corresponds to the choice of $\tilde{t} = 0$ for the moment of ejection (see Zhang et al. 2005 for the discussion of the “zero time effect”), and implies that the surface of the structured jet is slightly non-spherical during the flash.¹

For the emissivity in the comoving frame we assume:

$$I'_\nu(\theta) \propto (\nu_{\text{obs}} D)^{-\delta} \frac{\epsilon}{\Gamma} \quad \text{if } \Gamma(\theta) \geq 10 \quad (1)$$

$$I'_\nu(\theta) = 0 \quad \text{if } \Gamma(\theta) < 10 \quad (2)$$

where ν_{obs} is the observed frequency, $D = \Gamma^{-1}(1 - \vec{\beta} \cdot \hat{n})^{-1}$ is the Doppler factor, \hat{n} is a unit vector pointing toward the observer, ϵ is the energy of the outflow per unit solid angle, and $\Gamma = (1 - \beta^2)^{-1/2}$ is the bulk Lorentz factor of the outflow. The quantities ϵ and Γ in eq. (1) (and thereby β and D), all refer to the angle θ from the jet axis and the redshift $z = 0$ is assumed. The factor ϵ/Γ is introduced to represent the number of electrons at different viewing angles, i.e. $N_e(\theta) \propto \epsilon/\Gamma$.

The code is able to deal with any axially symmetric jet structure. After testing the code on the “top hat” jet case, we have made calculations for four jet structures:

1. gaussian, with

$$\epsilon(\theta) \propto \exp\left(-\frac{1}{2}\frac{\theta^2}{\theta_c^2}\right), \quad \Gamma(\theta) = 1 + (\Gamma_0 - 1) \exp\left(-\frac{1}{2}\frac{\theta^2}{\theta_c^2}\right), \quad (3)$$

¹ Complications introduced by the θ -dependent Lorentz factor are discussed in Section 3.4.

where $\Gamma_0 = \Gamma(\theta = 0)$ and θ_c is the characteristic width of the jet;

2. “e-gaussian” with $\epsilon(\theta)$ given by eq. (3) but with a fixed $\Gamma = \Gamma_0$ for all angles;

3. core + power law (hereafter CPL case):

$$\epsilon(\theta) \propto \left(1 + \frac{\theta^2}{\theta_c^2}\right)^{-a/2}, \quad \Gamma(\theta) = 1 + (\Gamma_0 - 1) \left(1 + \frac{\theta^2}{\theta_c^2}\right)^{-b/2}, \quad (4)$$

with $a = 2, b = 2$;

4. “e-CPL” case, which differs from CPL only in that Γ is fixed ($b = 0$ in eq. 4).

Thus, we consider two qualitatively different scenarios: cases 1 and 3 with both Γ and ϵ decreasing towards the edge of the jet according to (nearly) the same law, and cases 2 and 4 with ϵ decreasing, but Γ fixed. Note that in cases 1 and 3 the emissivity in the comoving frame is uniform since $\epsilon/\Gamma \approx \text{constant}$, as is in the top-hat case. The variations of Γ influence eq. (1) only through the Doppler factor D . Our calculation in the cases 1 and 3 is limited only to the relativistic part of the outflow (eq. 2).

3. RESULTS

Figs. 1a to 1d present our results obtained for $\Gamma_0 = 300$, $\theta_c = 5.7^\circ$, and $\delta = 1.3$. Different lightcurves, shown in the top panels, correspond to different viewing angles θ_{obs} . The solid and dotted lines correspond to the “on-beam” viewing ($\theta_{\text{obs}} = 0$ and $0.5\theta_c$, respectively). The short dashed line is for viewing along the edge of the bright jet core ($\theta_{\text{obs}} = \theta_c$), whereas the other lines are for “off-beam” viewing ($\theta_{\text{obs}} > \theta_c$).

3.1. The ubiquitous slope $2 + \delta$

The straight solid line in top panels marks the slope $2 + \delta = 3.3$, analytically predicted for a uniform outflow. It can be seen that regardless of the jet structure, majority of modeled lightcurves follows the $2 + \delta$ slope for many orders of magnitude in flux. The only exceptions are the lightcurves for off-beam viewing of a jet with Γ decreasing with distance from the jet axis (gaussian case, Fig. 1a, and CPL case, Fig. 1b). These off-beam lightcurves exhibit a break at a late time ($t \gtrsim 30$ s for the gaussian case, Fig. 1a, and $t \gtrsim 10^2$ s for the CPL case, Fig. 1b), after which the flux drops rapidly (on average following the slope ~ 3.8). The fast drop is caused by the lack of emission from the outer parts of the outflow (the jet edge given by eq. 2 starts to be visible for an observer).

The main reason for the trend to initially follow the $2 + \delta$ slope is that the decrease of flux due to the curvature effect occurs on a much shorter timescale than that for the jet structure to take effect. For the spectral index δ the flux decreases by m orders of magnitude after a time of $t_{\text{crv}} = 10^{m/(2+\delta)} t_{\text{off}}$, where t_{off} is the observer time at which the curvature effect began. For a typical $\delta \sim 1$, the flux drops by one-order of magnitude after a short time $t_{\text{crv}} \sim 2t_{\text{off}}$. A drop of three orders of magnitude occurs in no more than a decade in time. On the other hand, for

a spherical surface of the jet,² the observer can perceive the switch-off of emissivity at angle $\tilde{\theta}$ measured from the line of sight at a time $t_{\tilde{\theta}} \simeq [1 + (\tilde{\theta}\Gamma)^2]t_{\text{off}}$. One can see that the structure of the outflow must have the typical angular scale of the order of $3/\Gamma$ to affect the observed flux before $10t_{\text{off}}$. For $\Gamma_0 > 10^2$, the parameters of the outflow would have to vary strongly on a scale of one degree to be detectable at early time, when the flux is high. In both cases considered in this paper (i.e. gaussian and CPL), Γ changes little within the core of a jet, and this is why $\alpha \simeq 2 + \delta$ for $\theta_{\text{obs}} < \theta_c$. The strong deviation from $2 + \delta$ starts to be pronounced only when $\theta_{\text{obs}} \sim \theta_c \gg 1/\Gamma_0$, i.e. at late times or large viewing angles.

For a small core of angular radius $\theta_c = 1^\circ$ the discrepancy between the calculated slope and $2 + \delta$ appears at earlier time, as can be seen in Fig. 2.

3.2. Rebrightening

At late observational times the lightcurves diverge from the $2 + \delta$ slope, even in the “on beam” case. An interesting feature that appears for outflows with θ -dependent Lorentz factor is a rebrightening, visible for the gaussian case (Fig. 1a) at $t > 30$ s.

The reason for this behaviour is a nonmonotonic dependence of Doppler factor D on θ . After the sudden turn-off of emissivity, the observed flux decreases as $D^{(2+\delta)}$, and the Doppler factor can be approximated with $D_{\text{app}} = 2[\Gamma(\theta)]^{-1}\theta^{-2}$ in the limit of $\theta \gg 1/\Gamma$. Initially, the Lorentz factor changes slowly ($D_{\text{app}} \approx 2/(\Gamma_0\theta^2)$), so that D_{app} decreases with increasing θ (and t), and the flux follows the slope $2 + \delta$. As soon as $\theta(t) \sim \theta_c$, the factor $\Gamma(\theta)$ starts to decrease fast which initially slows down the rate of the flux decrease and the discrepancy from the slope $2 + \delta$ appears. Eventually, the decrease of $\Gamma(\theta)$ overcomes the dependence $D_{\text{app}} \propto \theta^{-2}$ and causes D_{app} (as well as the observed flux) to increase with time.

In the gaussian case (Fig. 1a) the flux reaches minimum when the observer receives radiation from $\theta = 2^{1/2}\theta_c$, which happens near $t \simeq 30$ s in Fig. 1a. The Lorentz factor at this angle is $\Gamma = 1 + (\Gamma_0 - 1)\exp(-1) \approx 111$ (for $\Gamma_0 = 300$ used throughout this paper).

In the CPL case shown in Fig. 1b the flux at $t \gtrsim 10^2$ s is nearly constant, because of the onset of the regime $\theta \gg \theta_c$, in which the specific structure of the outflow ($\Gamma(\theta) \propto \theta^{-2}$) cancels out the θ -dependence in $D_{\text{app}} \propto \Gamma^{-1}\theta^{-2}$. For the CPL case with a smaller core (Fig. 2) the levelling happens at earlier time ($t \sim 1$ s). After the plateau phase the lightcurve tends to steepen again³ before undergoing the jet edge break.

3.3. Role of the emission preceding the turn-off

The lightcurves with the rebrightening effect can be considered as consisting of two qualitatively different

² The front-surface of a jet with θ -dependent Lorentz factor should be non-spherical because the outflow velocity is not uniform. In the cases shown in Figs. 1 and 2, this effect is small and can be neglected (see Section 3.4).

³ The asymptotic slope which the lightcurve is trying to take on (but never succeeds because of the break) is equal to $\alpha = [\delta + 4 - (2/n)]/2$, where $n \geq 1$ is the exponent in the relation $\Gamma(\theta) \propto \theta^{-n}$ ($n = 2$ in the CPL case) and the convention $F_L \propto t^{-\alpha}$ was assumed. This temporal index corresponds to the limit $\theta \ll 1/\Gamma$.

parts: one of them has a power-law shape with a slope very close to $2 + \delta$; the other part, which includes the rebrightening, has a variable slope. This specific shape provides a good insight into the problem of how the shape of a lightcurve depends on the emissivity which preceded the turn-off.

We have numerically tested a variety of cases, assuming different duration of emission before the turn-off, and various radial dependence of the emissivity. We have found that the flux initially drops following the familiar $2 + \delta$ power-law, *independently on the emissivity that preceded the turn off*. However, the shape of a lightcurve in the region of the variable slope (especially in the valley preceding the rebrightening) is very sensitive to the duration, and to the time dependence of emissivity which preceded the turn-off (Fig. 3).

To understand this result, it is useful to consider the continuous emission preceding the turn-off, as consisting of a series of short flashes, each of which contributes its own lightcurve with the shape described above (power-law + rebrightening) but shifted horizontally with respect to each other and differently normalized. The observed lightcurve can then be considered to be a *sum* of these sub-lightcurves. In the period of time within which all these sub-lightcurves have the power-law shape (with the slope $2 + \delta$), the total lightcurve will have the same shape. In the region of the variable slope (near the rebrightening), the observed lightcurve takes on a different shape than the shape of individual components. Analogous effect happens when one calculates a photon spectrum by integrating over an electron energy distribution having a broken power-law shape.

Therefore, in the region of the non-power-law shape the lightcurves calculated for the short flash may differ noticeably from those calculated for the “sudden turn-off” case. Our choice of the “short flash” scenario has been mainly dictated by two facts: 1) The differences between the two cases in the non-power-law region are small if the emissivity preceding the turn-off increases quickly with time, or has a short duration. According to the internal shock model of GRBs (Rees & Mészáros 1994) both these conditions are likely to be fulfilled in reality. 2) A considerably larger number of model parameters is required to model the sudden switch-off case (e.g. the duration and the radial dependence of emissivity before the turn-off).

3.4. More realistic models

For an outflow with the θ -dependent Lorentz factor, the standard version of a curvature effect with the turn-off/flash occurring simultaneously at the same radial distance r_{off} from the central object is hardly conceivable, because of the non-uniform velocity of the outflow.

Therefore, we have also calculated lightcurves for a locally-short brightening of a spherical surface. The emission given by eq. (1) was limited to the region between $r_{\text{init}} = R_0$ and $1.05R_0$ and started non-simultaneously at a θ -dependent time $t_{\text{init}} = r/(\beta(\theta)c)$ (which may roughly correspond to a collision of a non-uniform outflow with a spherical layer of material).

Lightcurves calculated for such “non-simultaneous flash” at a fixed r are practically identical to those that we get for the simultaneous flash at the θ -dependent distance. This is because the additional radial delay $\Delta t_{\text{str}} = (r/c)[1 - v(\theta)/v(\theta = 0)]$ associated with the

extra curvature is much smaller than the standard delay for the spherical curvature: $\Delta t_{\text{sph}} = (r/c)[1 - \cos\theta]$. In other words, the reason is the proximity of $\beta(\theta)$ to 1 within the relativistic part of the outflow.

We next proceed to discuss the case of a flash at a place and time that correspond to a collision of two structured shells: a slow one, characterized by the Lorentz factor profile $\Gamma_s(\theta)$, and a fast one $[\Gamma_l(\theta)]$ ejected from the central source δt seconds later. For $t = 0$ corresponding to the ejection of the fast shell, the collision occurs at the time $\tilde{t}_{\text{col}}(\theta) = \delta t/(\beta_l(\theta)/\beta_s(\theta) - 1) \approx 2\delta t[\Gamma_s(\theta)]^2$ and at the radial distance $r_{\text{col}}(\theta) = \beta_l(\theta)\tilde{t}_{\text{col}}(\theta) \approx 2c\delta t[\Gamma_s(\theta)]^2$. Therefore, for outflows with Γ quickly decreasing with θ , as in the cases 1 and 3, the emission region is very elongated and has a pencil-like shape ($r_{\text{col}} \propto \Gamma_s^2$). Even at a large θ the radiation is emitted from $r_{\text{col}}(\theta) \ll r_{\text{col}}(\theta = 0)$, i.e. from regions located very close to the jet axis.

Surprisingly, however, the large additional distance that must be covered by photons does not produce large discrepancy from the $2 + \delta$ slope. The reason is that the collision at large θ occurs at much earlier time ($\tilde{t}_{\text{col}} \propto \Gamma_s^2$). This temporal advance $[\Delta t_t = \tilde{t}_{\text{col}}(0) - \tilde{t}_{\text{col}}(\theta)]$; hereafter (0) means ($\theta = 0$)] initially closely compensates the excess of the spatial delay caused by the additional curvature, which is $\Delta t_{\text{spt}} = r_{\text{col}}(0)/c - r_{\text{col}}(\theta)\cos(\theta)/c = \beta_l(0)\tilde{t}_{\text{col}}(0) - \beta_l(\theta)\tilde{t}_{\text{col}}(\theta)\cos(\theta)$. One can see that as long as $\Gamma_l(\theta) \gg 1$ and $\theta \lesssim \theta_c$ the difference between them is $\Delta t_{\text{spt}} - \Delta t_t \approx \Delta t_{\text{sph}}$, where $\Delta t_{\text{sph}} = r(0)[1 - \cos\theta]/c$ is the delay for the spherical curvature. The exact value of the temporal advance is slightly larger than the additional spatial delay ($\Delta t_t > \Delta t_{\text{spt}} - \Delta t_{\text{sph}}$), so that photons emitted there are actually observed *earlier* than in the case of the spherical outflow.

3.5. Outflow with the Lorentz factor independent of θ

In the cases with θ -independent Lorentz factor (Figs. 1c and 1d) the lightcurves initially follow the slope $2 + \delta$ and then behave in a way which is easy to interpret. For on-beam viewing ($\theta_{\text{obs}} \lesssim \theta_c$) the decline of flux is faster than $2 + \delta$, because the emissivity at a late time (larger angles θ) is weaker. For off-beam viewing ($\theta_{\text{obs}} > \theta_c$) the drop of flux becomes slower, because at the late time the bright core of the outflow becomes visible for the observer.

Unlike in the case of θ -dependent Lorentz factor, the problem of non-simultaneous turn-off does not arise in cases 2 and 4.

4. CONCLUSIONS

We have modeled the curvature effect in structured jet models. For “on-beam” viewing geometry, we find that the temporal decay slope, $2 + \delta$, as is derived for isotropic fireballs, is ubiquitous. The deviations happen in the “off-beam” geometry, with the line of sight pointing towards the Gaussian or power law wing of the structured jet. This gives a shallower decay index than $2 + \delta$.

Detailed analyses of *Swift* data indicate that in some cases, the rapid decay slopes of X-ray early afterglow lightcurves are somewhat shallower than $2 + \delta$ (O’Brien et al. 2005). One possible reason is that these reflect structured GRB jets viewed “off-beam”.

This work was supported by a research grant at UNLV

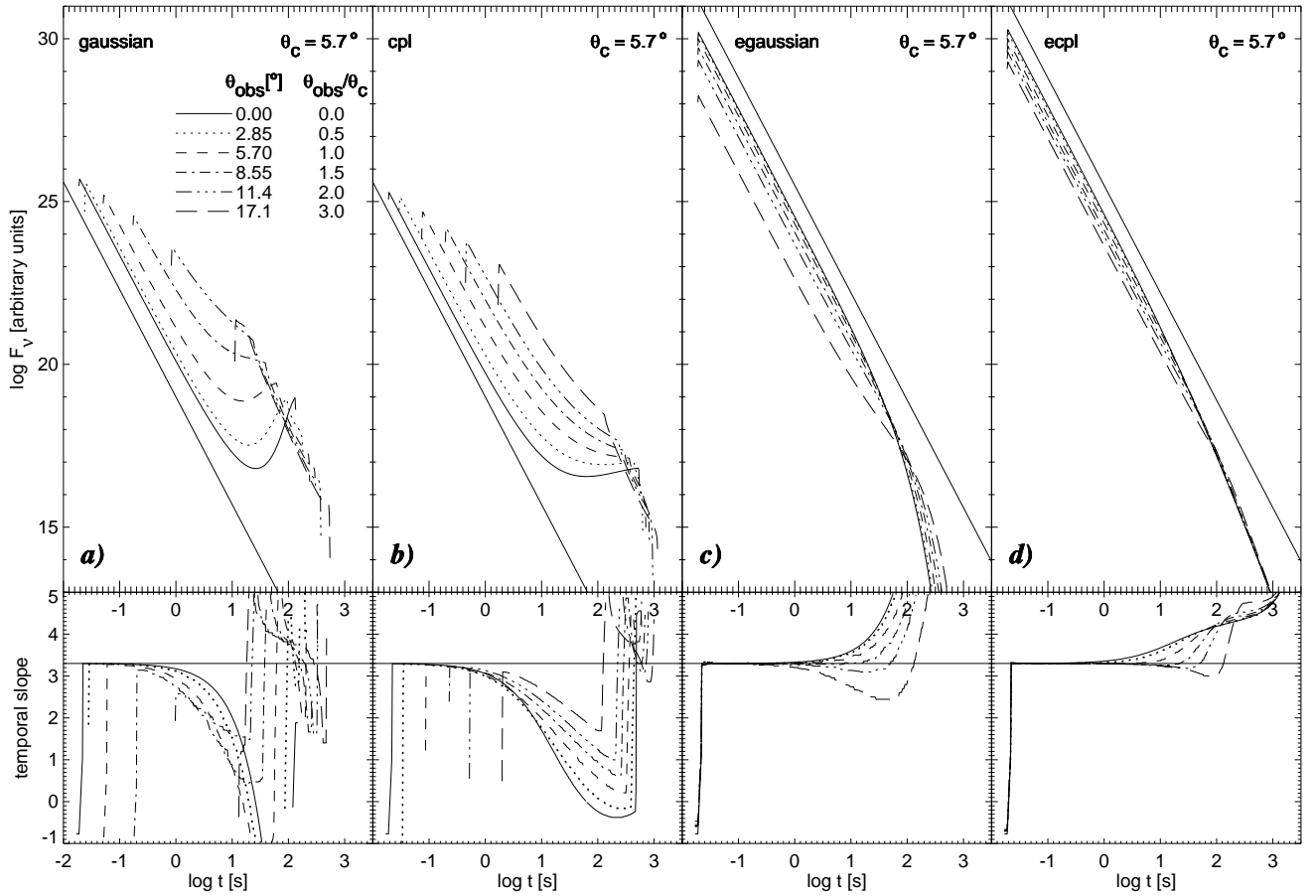


FIG. 1.— *Top*: Lightcurves for a short flash from a structured jet illustrating the curvature effect. Columns a), b), c) and d) refer to the structures described as cases 1, 2, 3, and 4 in Section 2. Different lines: solid, dotted, dashed, dot-dashed, dot-dot-dot-dashed, and long-dashed, correspond to the viewing angles $\theta_{\text{obs}}/\theta_c = 0, 0.5, 1, 1.5, 2$, and 3 , respectively. The straight solid line is for the analytically predicted slope $2 + \delta$. The result is for $\delta = 1.3$, $\theta_c = 5.7^\circ$, and $\Gamma_0 = 300$. *Bottom*: Temporal slope for the lightcurves in the top panel.

and by 2P03D.004.24 (JD) and by NASA under grants (BZ).
NNG05GB67G, NNG05GH92G, and NNG05GH91G

REFERENCES

- Burrows, D. N., Romano, P., Falcone, A., Kobayashi, S., Zhang, B. et al. 2005, *Science*, 309, 1833
Chincarini, G., Moretti, A., Romano, P., Covino, S., Tagliaferri, G., et al. 2005, *ApJ*, submitted (astro-ph/0506453)
Fan, Y. Z., & Wei, D. M. 2005, *MNRAS*, in press (astro-ph/0506155)
Granot, J., & Kumar, P. 2003, *ApJ*, 591, 1086
Kumar, P., & Granot, J. 2003, *ApJ*, 591, 1075
Kumar, P., & Panaitescu, A. 2000, *ApJ*, 541, L51
O'Brien, P., Willingale, R., Goad, M. R., Page, K. L. et al. 2005, to be submitted
Nousek, J. A., Kouveliotou, C., Grupe, D., Page, K. et al. 2005, *ApJ*, submitted (astro-ph/0508322)
Panaitescu, A., Mészáros, P., Gehrels, N., Burrows, D., & Nousek, J. 2005, *MNRAS*, submitted (astro-ph/0508340)
Rees, M. J., & Mészáros, P. 1994, *ApJ*, 430, L93
Rossi, E., Lazzati, D. & Rees, M. J. 2002, *MNRAS*, 332, 945
Salmonson, J. D. 2003, *ApJ*, 592, 1002
Tagliaferri, G., Goad, M., Chincarini, G., Moretti, A., Campana, S., et al. 2005, *Nature*, 436, 985
Wei, D. M. & Jin, Z. P. 2003, *A&A*, 400, 415
Yamazaki, R., Toma, K., Ioka, K. & Nakamura, T. 2005, *ApJ*, submitted (astro-ph/0509159)
Zhang, B., Dai, X., Lloyd-Ronning, N. M. & Mészáros, P. 2004, *ApJ*, 601, L119
Zhang, B., Fan, Y. Z., Dyks, J., Kobayashi, S., Mészáros, P., D. N. Burrows, J. A. Nousek, & N. Gehrels, 2005, *ApJ*, submitted (astro-ph/0508321)
Zhang, B. & Mészáros, P. 2002, *ApJ*, 571, 876

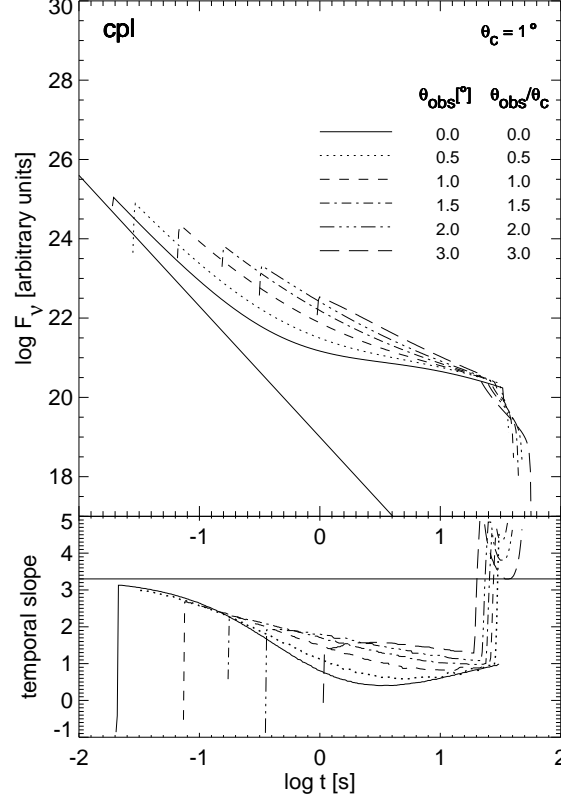


FIG. 2.— Same as in Fig. 1b (core + power law case) but for a significantly smaller core width $\theta_c = 1^\circ$.

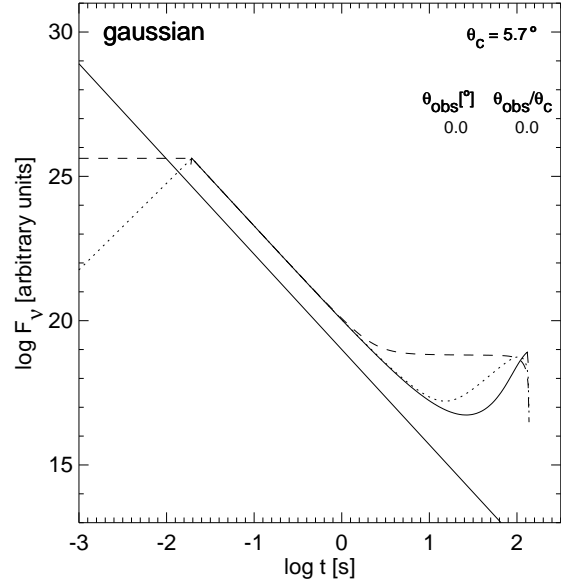


FIG. 3.— Comparison of a “short flash” lightcurve (solid curve) with lightcurves for the “sudden turn-off” case. The latter differ in a radial dependence of emissivity before the turn-off: the dotted line is for $I'_\nu \propto r^3$, and the dashed one is for $I'_\nu = \text{const}$. Note that the power-law part of the lightcurve after $t_{\text{off}} \approx 0.02$ s is not affected by the emission preceding the turn-off.